Inorg. Chem. **2003**, *42*, 8853–8865

Synthesis, Characterization, and Crystal Structure of the Pd(phen)(bdt) Complex. A DFT and TDDFT Study of Its Ground Electronic and Excited States Compared to Those of Analogous Complexes

Christodoulos Makedonas,[†] Christiana A. Mitsopoulou,*[,†] Fernando J. Lahoz,[‡] and Ana I. Balana[‡]

Inorganic Chemistry Laboratory, Department of Chemistry, National and Kapodistrian University of Athens, Panepistimiopolis, Zografou 15771, Greece, and Departamento de Quimica Inorganica—ICMA, Facultad de Ciencias, Universidad de Zaragoza—CSIC, 50009 Zaragoza, Spain

Received August 18, 2003

The synthesis and characterization of Pd(phen)(bdt) (**1**) (phen = 1,10-phenanthroline, bdt = 1,2-benzenedithiolate) is presented. **1** crystallizes in the monoclinic space group $P2_1/c$, $\alpha = 11.281(4)$ Å, $b = 20.498(8)$ Å, $c = 8.374(3)$ Å, $\beta = 90.234(8)$, $V = 1936.5(13)$ Å^3, $Z = 4$, and is isostructural with its previously reported related complexes. The ground and low lying excited electronic states in **1** and in the related complexes Pd(bpy)(bdt) (**2**), Pt(bpy)(bdt) (**3**), Pt(bpy)(mnt) (**4**), and Pt(bpy)(edt) (**5**) [where bpy = 2,2′-bipyridine, edt = ethylene-1,2-dithiolate, and mnt = maleonitriledithiolate] are studied using density functional theory techniques. The electronic properties of **1**–**5** are studied using the B3LYP functional. Optimized geometries are compared to experimentally observed structures. Time dependent density functional theory (TDDFT) is employed to investigate the excited singlet and triplet states. The calculated energies of the lowest singlet state and the lowest triplet state in all five complexes are in considerable agreement with experimental data. It is shown that variation of both metal and dithiolate-ligand going from **1** and **2** to **3**, **4**, and **5** has a substantial impact on the spectroscopic and excited-state properties, indicating at the same time the mixed metal/dithiolate character of the HOMO orbital. All the low-lying transitions are categorized as MMLL′CT transitions. The emissive state of all complexes is assigned as a triplet dithiolate/metal to diimine charge transfer with differences in the structures of the emissions resulting from differences in the π^* dithiolate orbital of the mnt, bdt, and edt as well as from differences in metal.

Introduction

Over the last three decades M(diimine)(dithiolate) complexes of group VIII metals have attracted the interest of numerous researchers because of their unique properties, which include solution luminescence, solvatochromism, large molecular hyperolarizabilities, and large excited-state oxidation potentials.[1−5] In the meantime, nonlinear optical (NLO) materials have also attracted great interest because of their wide range of possible applications in several fields, such as laser technology, telecommunications, data storage, and optical switches.[6] The above-mentioned complexes with the "noninnocent" dithiolene ligand represent a very promising class of compounds for NLO materials, in view of their peculiar electronic structure. This specific structure is dominated by the existence in the same molecule of the two different unsaturated chelating ligands, one of which is more easily reduced and the other more easily oxidized. These complexes generally absorb light in the visible and ultraviolet regions. Over the past decade, Eisenberg and co-workers have performed elaborate studies on the charge-transfer excited state of mixed-ligand Pt(II) complexes with diimine and dithiolate ligands. For most complexes, the excited state is considered to involve the highest occupied molecular orbital (HOMO), which is a mixture of platinum and dithiolate orbital character, and the lowest unoccupied molecular orbital (LUMO), which is a π^* orbital of the diimine and has been termed a "mixed-metal/ligand-to-ligand charge transfer" (MMLL′CT).[2k] The square planar geometry of platinum (II) complexes with α-diimine ligands makes it feasible to introduce selectively properly designed α-diimine

* Author to whom correspondence should be addressed. E-mail: mitsopoulou@chem.uoa.gr.
[†] National and Kapodistrian University of Athens.
[‡] Universidad de Zaragoza.

(1) Miller, T. R.; Dance, I. G. *J. Am. Chem. Soc.* **1973**, *95*, 6970−6979.

10.1021/ic034978j CCC: $25.00
Published on Web 11/15/2003

ligands and suitable coligands in a coplanar arrangement and thus allows the tailoring of molecules for potential application as photosensitizers or photocatalysts. Electronic transitions in such complexes span a broad range depending on both the diimine ligands and the coligands.[2] The charge transfer excited state of Pt(II) complexes is emissive, in contradiction to Pd(II), in fluid solution and undergoes electron-transfer quenching both oxidatively and reductively.[2c,f,i−l,r,s] In 1985 Srivastava and co-workers suggested that both complexes Pt(bpy)(tdt) and Pd(bpy)(tdt) act as photosensitizers for the formation of singlet oxygen, attributing this ability to a unique LL′CT-based excited state.[4b] More recently, attention has again shifted to the mixed ligand complexes of Pd(II) and Pt(II) as they undergo photoinduced oxidation in the presence of atmospheric oxygen to yield monosulfenate, disulfenate, mixed sulfinate/sulfenate, monosulfinate, and disulfinate complexes.[4a,c,7] Moreover all these years the intense solvatochromic band in the visible region of their electronic spectra has been assigned as interligand charge transfer (LL′CT)[1], mixed metal/ligand to ligand (MMLL′CT),[2k] or more generally as charge transfer to ligand transition.[2g,2i]

Recalling our knowledge for the nature of the transitions, we can state that the "classical" metal-to-ligand charge transfer (MLCT) transition is attributed to the electronic transition $d \rightarrow \pi^*$, where π^* is the antibonding orbital of the diimine ligand, a good π acceptor. In the case that coligands are no longer innocent, but provide high lying filled p or π orbitals, the HOMO may have significant to dominating coligand contributions, admixed to metal *n*d orbitals, and the resulting lowest transition is assigned to a ligand-to-ligand charge transfer (LL′CT).[4h] Since the HOMO has mixed metal/ligand character, it is also referred to as mixed metal/ligand to ligand charge transfer (MMLL′CT).[2f]

From this point of view we can assign the main difference between the LL′CT and MMLL′CT transitions as the percentage of metal *n*d orbitals to HOMO. Since in the literature both assignments have been considered for the lowest energy transition of M(diimine)(dithiolate) complexes along with the nonspecific term "charge transfer to diimine" transition that has been employed by Eisenberg et al. more recently,[2g,i] it seems that the knowledge of the nature of the frontier orbitals as well as the nature of the energy transitions would be unambiguously a helpful tool in synthesis or design of functional molecules and for a mechanistic analysis of their photochemistry and electrochemistry. An appropriate choice of diimine chelate ligand, metal, and coligand (dithiolene or dithiolate) should therefore allow predetermination of the character of the lowest energy transitions and lowest emitting states in such molecules. Up to now the assignments of their excited state are based mainly on the pioneering experimental work of Eisenberg,[2] as complemented by elementary theoretical work on frontier orbitals.[2n] Despite the fact that DFT calculations have been performed on dithiolene or diimine complexes, to our knowledge, there is no report on planar mixed ligand dithiolate−diimine complexes. As DFT has been proven to be extremely useful to obtain more accurate molecular orbital energies and other properties of transition metals complexes,[8] there is no doubt that such a study would be beneficial.

This paper reports a combined experimental and theoretical study including absorption and emission spectroscopy along with quantum chemical calculations (by means of DFT formalism) to determine the character of electronic transitions in a series of electron rich palladium and platinum complexes of the type M(diimine)(dithiolate) with diimine = bpy and phen and dithiolate = mnt^{2-}, bdt^{2-}, and edt^{2-}. The main

(2) (a) Huertas, S.; Hissler, M.; McGarrah, J. E.; Lachicotte, R. J.; Eisenberg R. *Inorg. Chem.* **2001**, *40*, 1183−1188. (b) Hissler, M.; McGarrah, I. E.; Connick, W. B.; Geiger, D. K.; Cummings, S. D.; Eisenberg, R. *Coord. Chem. Rev.* **2000**, *208*, 115−137. (c) Connick, W. B.; Geiger, D.; Eisenberg, R. *Inorg. Chem.* **1999**, *38*, 3264−3265. (d) Mansour, M. A.; Lachicotte, R. J.; Gysling, H. J.; Eisenberg, R. *Inorg. Chem.* **1998**, *37*, 4625−4632. (e) Paw, W.; Lachicotte, R. J.; Eisenberg, R. *Inorg. Chem.* **1998**, *37*, 4139−4141. (f) Paw, W.; Cummings, S. D.; Mansour, M. A.; Connick, W. B.; Geiger, D. K., Eisenberg, R. *Coord. Chem. Rev.* **1998**, *171*, 125−150. (g) Cummings, S. D.; Cheng, L.-T.; Eisenberg, R. *Chem. Mater.* **1997**, *9*, 440−450. (h) Paw, W.; Eisenberg, R. *Inorg. Chem.* **1997**, *36*, 2287−2293. (i) Cummings, S. D.; Eisenberg, R. *J. Am. Chem. Soc.* **1996**, *118*, 1949−1960. Pt(NN)(SS) solvent parameters: CCl_4 (0.000), toluene (0.172), benzene (0.218), THF (0.494), chloroform (0.610), 3-pentane (0.676), pyridine (0.743), 1,2-dichloroethane (0.758), dichloromethane (0.765), acetone (0.797), DMF (0.901), DMSO (0.973), acetonitrile (1.000). (j) Cummings, S. D.; Eisenberg, R. *Inorg. Chem.* **1995**, *34*, 3396−3404. (k) Cummings, S. D.; Eisenberg, R. *Inorg. Chem.* **1995**, *34*, 2007−2014. (l) Bevilacqua, J. M.; Eisenberg, R. *Inorg. Chem.* **1994**, *33*, 1886−1890. (m) Bevilacqua, J. M.; Eisenberg, R. *Inorg. Chem.* **1994**, *33*, 2913−2923. (n) Zuleta, J. A.; Bevilacqua, J. M.; Proserpio, D. M.; Harvey, P. D.; Eisenberg, R. *Inorg. Chem.* **1992**, *31*, 2396−2404. (o) Zuleta, J. A.; Bevilacqua, J. M.; Rehm, J. M.; Eisenberg, R. *Inorg. Chem.* **1992**, *31*, 1332−1337. (p) Zuleta, J. A.; Bevilacqua, J. M.; Eisenberg, R. *Coord. Chem. Rev.* **1992**, *111*, 237−248. (q) Zuleta, J. A.; Burberry, M. S.; Eisenberg, R. *Coord. Chem. Rev.* **1991**, *111*, 237−248. (r) Zuleta, J. A.; Burberry, M. S.; Eisenberg, R. *Coord. Chem. Rev.* **1990**, *97*, 47−64. (s) Zuleta, J. A.; Chesta, C. A.; Eisenberg, R. *J. Am. Chem. Soc.* **1989**, *111*, 8916−8917.

(3) (a) Kubo, K.; Nakano, M.; Tamura, H.; Matsubayashi, G.-E. *Inorg. Chem. Acta* **2002**, *336*, 120−124. (b) Matsubayashi, G.; Nakano, M.; Tamura, H. *Coord. Chem. Rev.* **2002**, *226*, 143−151. (c) Islam, A.; Sugihara, H.; Hara, K.; Singh, L. P.; Katoh, R.; Yanakida, M.; Takahashi, Y.; Murata, S.; Arakawa, H. *Inorg. Chem.* **2001**, *40*, 5371−5380. (d) Islam, A.; Sugihara, H.; Hara, K.; Singh, L. P.; Katoh, R.; Yanakida, M.; Takahashi, Y.; Murata, S.; Arakawa, H. *J. Photochem. Photobiol. A: Chem.* **2001**, *145*, 135−141. (e) Islam, A.; Sugihara, H.; Hara, K.; Singh, L. P.; Katoh, R.; Yanakida, M.; Takahashi, Y.; Murata, S.; Arakawa, H. *New J. Chem.* **2000**, *24*, 343−345. (f) Natsuaki, K.; Nakano, M.; Matsubayashi, G.-E.; Arakawa R. *Inorg. Chem. Acta* **2000**, *299*, 112−117. (g) Chen, C. T.; Liao, S.-Y.; Lin, K.-J.; Chen, C.-H.; Lin, T.-Y. J. *Inorg. Chem.* **1999**, *38*, 2734−2741. (h) Chen, C. T.; Liao, S.-Y.; Lin, K.-J.; Lai, L.-L. *Adv. Mater.* **1998**, *10*, 334−338. (i) Chen, C. T.; Lin, T.-Y. J.; Chen, C.-H.; Lin, K.-J. *J. Chin. Chem. Soc.* **2000**, *47*, 197−201. (j) Matsubayashi, G.-E.; Yamaguchi, Y.; Tanaka, T. *J. Chem. Soc., Dalton Trans.* **1988**, 2215.

(4) (a) Kaasjager, V. E.; Bouwman, E.; Gorter, S.; Reedijk, J.; Grapperhaus, C. A.; Reibenspies, J. H.; Smee, J. J.; Darensbourg, M. Y.; Derecskei-Kovacs, A.; Thomson, L. M. *Inorg. Chem.* **2002**, *41*, 1837−1844. (b) Puthraya, K. H.; Srivastava, T. S. *Tetrahedron* **1985**, *4*, 1579−1584. (c) Zhang, Y.; Ley, K. D.; Schanze, K. S. *Inorg. Chem.* **1996**, *35*, 7102−7110. (d) Base, K.; Tierney, M. T.; Fort, A.; Muller, J.; Grinstaff, M. W. *Inorg. Chem.* **1999**, *38*, 287−289. (e) Base, K.; Grinstaff, M. W. *Inorg. Chem.* **1998**, *37*, 1432−1435. (f) Si, J.; Yang, Q.; Wang, Y.; Ye, P.; Wang, S.; Qin, J.; Lin, D. *Optics Commun.* **1996**, *132*, 311−315. (g) Vicente, R.; Ribas, J.; Cassoux, P.; Sourisseau, C. *Synth. Met.* **1986**, *15*, 79−89. (h) Vogler, A.; Kunkely, H. *Comments Inorg. Chem.* **1990**, *9*, 201−220. (i) Vogler, A.; Kunkely, H. *J. Am. Chem. Soc.* **1981**, *103*, 1559−1560.

(5) (a) Makedonas, C.; Mitsopoulou, C. *J. Inorg. Biochem.* **2001**, *86*, 326. (b) Makedonas, C.; Mitsopoulou, C. *ICCC35*, Heidelberg, July 2002. (c) Makedonas, C.; Mitsopoulou, C. *FIGIPS7*, Lisbon, June 2003.

(6) Zyss, J., Ed. *Molecular Nonlinear Optics*; Academic Press: Boston, MA, 1993.

(7) (a) Cocker, T. M.; Bachman, R. E. *Inorg. Chem.* **2001**, *40*, 1550−1556. (b) Connick, W. B., Gray, H. B. *J. Am. Chem. Soc.* **1997**, *119*, 11620−11627.

objective was to ascertain, first, the extent to which the coligands and metal contribute to the frontier orbitals and hence to the excited state and, second, whether emission spectroscopy can give a clue as to the excited-state character. The synthesis and characterization of the Pd(phen)(bdt) complex (**1**) is reported. The electronic structures of **1**, Pd(bpy)(bdt) (**2**), Pt(bpy)(bdt) (**3**), Pt(bpy)(mnt) (**4**), and Pt(bpy)(edt) (**5**) are elucidated. The emission assignments reported below are based on experimental arguments, accumulated both here and in the literature, and on calculations of the energies and characters of low-lying triplet excited states, using time-dependent density functional theory (TD-DFT). Although TDDFT technique has been widely applied to evaluate the singlet excited state of a large number of compounds, to our knowledge, there are just a few papers where TDDFT triplet calculations have been used to establish an interpretation of photophysical properties of metal complexes.[9]

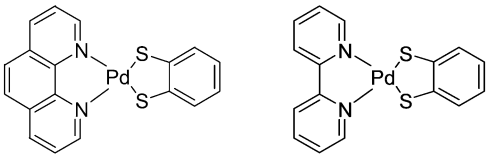

Pd(phen) (bdt) **(1)**

Pd(bpy) (bdt) **(2)**

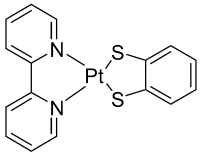

Pt(bpy) (bdt) **(3)**

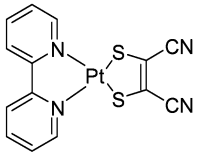

Pt (bpy) (mnt) **(4)**

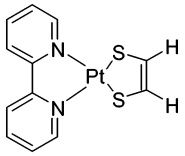

Pt (bpy) (edt) **(5)**

1. Experimental Section

1.1. Preparation of Compounds. All reactions and manipulations were conducted under a pure argon atmosphere using standard Schlenk techniques. Solvents were purified prior to use by standard procedures.[10] The chemicals phen, bpy, $Pd(phen)Cl_2$, $Pt(bpy)Cl_2$, H_2bdt, and $Na_2mnt{\cdot}2H_2O$ were purchased by Aldrich and used as received. The compounds $Pt(bpy)(mnt)$[2r], Pt(bpy)(bdt),[7] Pt(bpy)(edt),[11] Pd(bpy)(bdt),[7a] and H_2edt[11] were prepared according to literature procedures. Their physical properties are consistent with those reported.

Synthesis of Pd(phen)(bdt). H_2bdt (0.75 mL, 0.65 mmol) was added to a 15 mL methanol solution of 0.093 g (1.60 mmol) KOH and stirred for 20 min. The resulting solution was added to a stirring suspension of 225.06 mg (0.629 mmol) $Pd(phen)Cl_2$. The solution turned instantly from yellow to deep red and was left to stir for 24 h under room temperature. Then 200 mL of ice−water was added to the red solution, and the resulting suspension was cooled to 4 °C for 24 h. A deep red precipitate was collected after filtration and washed several times with small amounts of methanol and diethyl ether. Deep red needles were obtained by recrystallization during slow evaporation from a concentrated DMSO solution at 298 K.

Yield: 190.70 mg (71%). ^{1}H NMR (ppm): 6.81 (dd, H4−5(bdt), $J_1 = 3.3$ Hz, $J_2 = 5.9$ Hz), 7.05 (dd, H3−6(bdt), $J_1 = 3.3$ Hz, $J_2 = 5.9$ Hz), 8.13 (dd, H3−8(phen), $J_1 = 5.1$ Hz, $J_2 = 8.0$ Hz) 8.28 (s, H5−6(phen)), 8.93 (dd, H4−7(phen), $J_1 = 1.5$ Hz, $J_2 = 8.0$ Hz), 9.01 (dd, H2−9(phen), $J_1 = 1.5$ Hz, $J_2 = 5.1$ Hz). ^{1}H NMR ($CDCl_3$, ppm): 6.83 (dd, 2H), 7.12 (dd, 2H), 7.79 (dd, 2H), 7.90 (s, 2H), 8.44 (dd, 2H,), 9.14 (dd, 2H).

Absorption spectrum: λ_{max}(DMSO) = 485 nm ($\epsilon = 3200$ M^{-1} cm^{-1}) λ_{max} ($CHCl_3$) = 531 nm, λ_{max}(THF) = 548 nm. FT-IR spectrum: 667 cm^{-1} (in plane def.—bdt ring), 714 cm^{-1} (w(C−H, phen)), 736 cm^{-1} (w(C−H, bdt)).

High-resolution MS(ESI), exact mass calculated for $[C_{18}H_{12}N_2PdS_2]^+$ (M^+): 426.85. Found: 426.84 Anal. Calcd for $C_{18}H_{12}N_2PdS_2$: C 50.65; H 2.83; N 6.56; S 15.02. Found: C 50.32; H 2.58; N 6.74; S 14.58.

1.2. Physical Measurements. ^{1}H NMR spectra were obtained on a Varian UNITYplus operating at 300 MHz spectrometer with chemical shifts reported in ppm downfield from tetramethylsilane (TMS), using the solvent peaks as an internal reference. Absorption spectra were determined with a Varian Cary 300 spectrophotometer.

FT-IR spectra were recorded on a Nicolet Magna IR 560 spectrophotometer. High-resolution mass spectra were obtained on a mass spectrometer using electron spray ionization (ESI). Elemental analysis was performed on a Euro EA3000 Series Euro Vector CHNS elemental analyzer. Luminescence spectra were recorded on a Perkin-Elmer LS-50B fluorometer and the Edinburgh Instruments model FS spectrofluorometer. Glassy 77 K solutions were obtained in 1:1:1 DMSO:dichloromethane:methanol (abbreviated as DMM).

1.3. X-ray Structure Determination for 1. All crystallization processes gave rise to narrow needles that easily formed different sized aggregates. A red needle (0.231 × 0.032 × 0.026 mm) was used for data collection. Intensity measurements were made using a Bruker Smart APEX CCD diffractometer at 100(2) K with Mo Kα radiation and graphite monochromator. A total of 7985 reflections were collected ($\theta = 1.8-22.6°$; $\omega/2\theta$ scans); of these 2517 were unique ($R_{int} = 0.0669$ ($I > 2\sigma(I)$). The structure was solved by Patterson and difference Fourier methods, and refined using SHELXTL (weighting scheme $w^{-1} = \sigma^2(F_o^2) + (0.0850P)^2$, where $P = [\max(F_o^2 + 2F_c^2)]/3$).[12] All non-hydrogen atoms of the complex were refined anisotropically. Hydrogen atoms were found in calculated positions and refined riding on their carbon atoms

(8) (a) Lauterbach, C.; Fabian, J. *Eur. J. Inorg. Chem.* **1999**, 1995−2004. (b) Lim, B. S.; Fomitchev, D. V.; Holm, R. H. *Inorg. Chem.* **2001**, *40*, 4257−4262. (c) Farrell, I. R.; František, H.; Záliš, S.; Mahabiersing, T.; Vlček, A., Jr. *J. Chem. Soc., Dalton Trans.* **2000**, 4323−4331. (d) Fomitchev, D. V.; Lim, B. S.; Holm, R. H. *Inorg. Chem.* **2001**, *40*, 645−654. (e) Tobisch, S.; Nowak, T.; Bogel, H. *J. Organomet. Chem.* **2001**, *619*, 24−30. (f) van Slageren, J.; Stufkens D. J.; Záliš, S.; Klein, A.; *J. Chem. Soc., Dalton Trans.* **2002**, 218−225.

(9) (a) Farrell, I. R.; van Slageren, J.; Záliš, S.; Vlček, A., Jr. *Inorg. Chim. Acta* **2001**, *315*, 44−52. (b) Hay, P. J. *J. Phys. Chem. A* **2002**, *106*, 1634−1641. (c) Guillemoles, J. F.; Barone, V.; Joubert, L.; Adamo, C. *J. Phys. Chem. A* **2002**, *106*, 11354−11360. (d) Monat, J. E.; Rodriguez, J. H.; McCusker, J. K. *J. Phys. Chem. A* **2002**, *106*, 7399−7406.

(10) Perrin, D. D.; Armarego, W. L. F. *Purification of Laboratory Chemicals*, 3rd ed.; Pergamon Press: New York, 1988.

(11) Keefer, C. E.; Bereman, R. D.; Purrington, S. T.; Knight, B. W.; Boyle, P. D. *Inorg. Chem.* **1999**, *38*, 2294−2302.

(12) Sheldrick, G. M. *SHELXTL 97*; University of Göttingen: Göttingen, 1997.

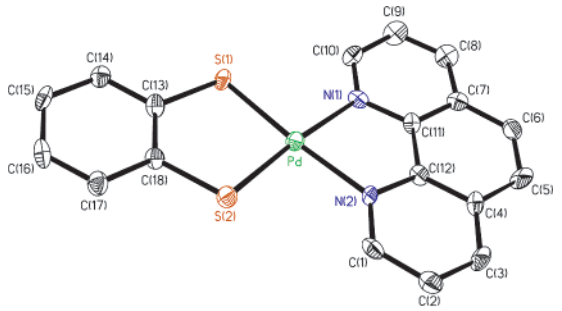

Figure 1. Molecular structure and atom numbering (ORTEP diagram, 50% thermal ellipsoids) of **1**.

Table 1. Crystallogaphic Data for **1**

cryst data	Pd(phen)(bdt)·dmso
empirical formula	$C_{20}H_{12}N_2OPdS_3$[a]
fw, g mol^{-1}	504.94
cryst syst	*monoclinic*
space group	$P2_1/c$ (No. 14)
a, Å	11.281(4)
b, Å	20.498(8)
c, Å	8.374(3)
β, deg	90.234(8)
V, Å^3	1936.5(13)
Z	4
λ, Å	0.71073
T, K	100(2)
R1[b]	0.0669
wR2[b]	0.1495
GOF (F^2)[b]	1.051

[a] A solvent molecule (DMSO) was crystallized with the complex. [b] R1 = $\sum||F_o| - |F_c||/\sum|F_o|$ (2517 observed reflections, $I > 2\sigma(I)$); wR2 = $[\sum[w|F_o^2 - F_c^2|^2]/w(F_o^2)^2]^{1/2}$; GOF = $[\sum[w|F_o^2 - F_c^2|^2]/(n-p)]^{1/2}$, where n is the number of data and p is the number of parameters refined.

with two common thermal parameters. The structure and numbering scheme of the atoms of the complex are presented in Figure 1. Table 1 contains the crystal data of the complex. The complex was cocrystallized with a solvent molecule.

1.4. Computational Details. Ground-state electronic structure calculations of **1**−**5** complexes have been performed using density functional theory (DFT)[13] methods employing the GAUSSIAN 98 software package.[14] The functional used throughout this study is the B3LYP, consisting of non local hybrid exchange functional as defined by Becke's three-parameter equation[15] and the non local Lee−Yang−Parr correlation functional.[16] The ground-state geometries were obtained in the gas phase by full geometry optimization, starting from structural data, regularized in order to satisfy the C_{2v} symmetry. The VeryTight option was used in all cases, which demands tighter convergence criteria than the default ones, while numerical integration was performed using the UltraFine option, which requests a pruned (99,590) grid. The optimum structures located as saddle points on the potential energy surfaces were verified by the absence of imaginary frequencies. The derived wave functions were found free of internal instabilities. The basis set used for all nonmetal atoms was the well-known valence triple-ζ 6-311+G*.[17] The quasi-relativistic Stuttgardt−Dresden effective core potential of the type ECP28MWB and ECP60MWB was used for Pd and Pt, respectively.[18] The core potentials were complemented by the relative valence basis sets.[18] For all other calculations related to the properties investigation, an additional diffuse and polarization function was added to the hydrogen atoms. Preliminary calculations indicated that the addition of a p-type polarization function to the metals' valence basis sets[8a] produced practically the same results; general application of it was not selected to avoid further computational cost. The 16 to 18 lowest singlet and triplet excited states of the closed shell complexes were calculated within the TDDFT formalism as implemented in Gaussian.[19] Percentage compositions of molecular orbitals from the three contributing fragments were calculated using the AOMix progam.[20a,b] Finally, percentage of different transitions contributing to a state was calculated with the aid of SWizard.[20b,c] To estimate the possible response of electronic structure due to the solvation, the solvent was modeled by the polarizable continuum model (PCM) implemented in G98.[21]

2. Results and Discussion

2.1. Molecular Structure. The red complex Pd(phen)(bdt) **(1)** has been prepared in high yield from Pd(phen)Cl_2 and H_2bdt in the presence of base, eq 1. This complex was

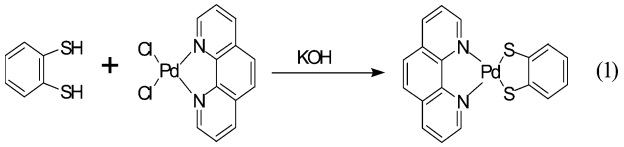

(1)

characterized by elemental analysis, ES-MS, ^{1}H NMR, electronic spectroscopies, and single-crystal X-ray diffraction. The ORTEP diagram of **1**·dmso, including the numbering system, obtained from the crystal structure analysis is shown in Figure 1, while selected bond lengths and angles for the

(13) Parr, R. G.; Yang, W. *Density Functional Theory of Atoms and Molecules*; Oxford University Press: Oxford, 1989.
(14) Frisch, M. J.; Trucks, G. W.; Schlegel, H. B.; Scuseria, G. E.; Robb, M. A.; Cheeseman, J. R.; Zakrzewski, V. G.; Montgomery, J. A., Jr.; Stratmann, R. E.; Burant, J. C.; Dapprich, S.; Millam, J. M.; Daniels, A. D.; Kudin, K. N.; Strain, M. C.; Farkas, O.; Tomasi, J.; Barone, V.; Cossi, M.; Cammi, R.; Mennucci, B.; Pomelli, C.; Adamo, C.; Clifford, S.; Ochterski, J.; Petersson, G. A.; Ayala, P. Y.; Cui, Q.; Morokuma, K.; Malick, D. K.; Rabuck, A. D.; Raghavachari, K.; Foresman, J. B.; Cioslowski, J.; Ortiz, J. V.; Stefanov, B. B.; Liu, G.; Liashenko, A.; Piskorz, P.; Komaromi, I.; Gomperts, R.; Martin, R. L.; Fox, D. J.; Keith, T.; Al-Laham, M. A.; Peng, C. Y.; Nanayakkara, A.; Gonzalez, C.; Challacombe, M.; Gill, P. M. W.; Johnson, B. G.; Chen, W.; Wong, M. W.; Andres, J. L.; Head-Gordon, M.; Replogle, E. S.; Pople, J. A. *Gaussian 98*, revision A.9; Gaussian, Inc.: Pittsburgh, PA, 1998.
(15) Becke, A. D. *J. Chem. Phys.* **1993**, *98*, 5648−5652.
(16) Lee, C.; Yang, W.; Parr, R. G. *Phys. Rev. B* **1988**, *37*, 785−789.
(17) (a) McLean, A. D.; Chandler, G. S. *J. Chem. Phys.* **1980**, *72*, 5639−5648. (b) Krishnan, R.; Binkley, J. S.; Seeyer, R.; Pople, J. A. *J. Chem. Phys.* **1980**, *72*, 650−654.
(18) Andrae, D.; Haeussermann, U.; Dolg, M.; Stoll, H.; Preuss, H. *Theor. Chim. Acta* **1990**, *77*, 123−141.
(19) Stratmann, R.; Scuseria, G.; Frisch, M. *J. Chem. Phys.* **1998**, *109*, 8218−8224.
(20) (a) Gorelsky, S. I. *AOMix progam*, revisions 4.7 and 5.1, http://www.obbligato.com/software/aomix/ (accessed July 2002). (b) Gorelsky, S. I.; Lever, A. B. P. *J. Organomet. Chem.* **2001**, *635*, 187−196. (c) Gorelsky, S. I. *SWizard progam*, http://www.obbligato.com/software/swizard/ (accessed July 2002).
(21) Barone, V.; Cossi, M. *J. Phys. Chem. A* **1998**, *102*, 1995−2001.
(22) Schriver, D. F.; Atkins, P. W. *Inorganic Chemistry*, 3rd ed., W. H. Freeman and Co: New York, 1999; pp 23−26.
(23) (a) Janiak, C. *J. Chem. Soc., Dalton Trans.* **2000**, 3885−3896. (b) Flleman, W. L.; Connick, W. B. *Comments Inorg Chem*, **2002**, *23*, 205−230. (c) Smucker, B. W.; Hudson, J. M.; Omary, M. A.; Dunbar, K. R. *Inorg. Chem.* **2003**, *42*, 4714−4723.
(24) Argyropoulos, D. Lyris, E.; Mitsopoulou, C. A.; Katakis, D. *J. Chem. Soc., Dalton Trans.* **1997**, 615−621 and references therein.
(25) (a) Kosower, E. *J. Am. Chem. Soc.* **1958**, *80*, 3253−3260. (b) Manuta, D. M.; Lees, A. J. *Inorg. Chem.* **1986**, *25*, 1354−1359. (c) Reichardt, C. *Angew. Chem., Int. Ed. Engl.* **1965**, *4*, 29−39.
(26) Stowasser, R.; Hoffmann, R. *J. Am. Chem. Soc.* **1999**, *121*, 3414−3420.

Table 2. Selected Bond Lengths (Å) and Angles (deg) for **1** with Atom Labels According to Figure 1, with Estimated Standard Deviations in Parentheses

bonds		angles	
Pd1−N1	2.089(8)	N1−Pd1−N2	80.2(3)
Pd1−N2	2.103(8)	S2−Pd1−S1	89.17(10)
Pd1−S1	2.267(3)	N1−Pd1−S1	95.5(2)
Pd1−S2	2.254(3)	N2−Pd1−S2	95.1(2)
N1−C11	1.379(12)	N1−Pd1−S2	175.3(2)
N2−C12	1.356(12)	N2−Pd1−S1	175.6(2)
C11−C12	1.437(13)	C11−N1−Pd1	112.2(6)
S1−C13	1.779(10)	C12−N2−Pd1	112.5(6)
S2−C18	1.794(10)	C13−S1−Pd1	105.2(3)
C13−C18	1.376(13)	C18−S2−Pd1	105.2(3)
N1−C10	1.323(12)	C10−N1−Pd1	129.7(7)
N2−C1	1.344(12)	C1−N2−Pd1	128.5(7)

structure are given in Table 2. Although a few crystal structures of Pt(II)(diimine)(dithiolate) complexes have been reported, there is only one reference on analogous complexes of Pd(II) and its mono- and disulfonate derivatives.[7a] Thus, herein the second crystal structure of a Pd(II) analogous complex is presented. Complex **1** possesses square planar coordination geometry with the two five membered rings lying on the same plane. The Pd−N distances of 2.096(8) and the N−Pd−N bond angle of 80.2(3)° agree well with the values found for **2** (Table 3), according to the less π^* back-bonding of phen, but they are slightly longer than those observed in the Pt(II) complexes (average value 2.050 Å). The observed Pd−S distances are in close agreement between **1**, **3**,[7a] and **5**. The Pd−S distances of 2.254(3) and 2.267(3) Å are essentially equal to the average value of 2.250 Å reported for **3**[7b] and for analogous dithiolene complexes,[2m] in keeping with the similar bonding radii of the second-and third-row transition metals.[22] On one hand, the identity of the metal atom does not seem to have a large structural influence on the dithiolate ligand because the C−S bond lengths are essentially identical (**2** = 1.762(2) Å and **3** = 1.761(6) Å); on the other, the nature of the diimine ligand affects this bond length, therefore the distance of C−S in complex **2** is slightly shorter (1.762(2) Å) as compared to the one of **1** (1.787(10) Å).

Intermolecular interactions are of importance for optical spectroscopy.[23a] Therefore we examine the crystal structure of complex **1** in that respect. In square-planar platinum(II) complexes, two intermolecular interactions are important, namely, π interactions of the aromatic α-diimine ligands and Pt···Pt interactions.[23b,c]

In fact complex **1** exhibits quite a complex stacking behavior (Figure 2A). It is stacked in two different columns

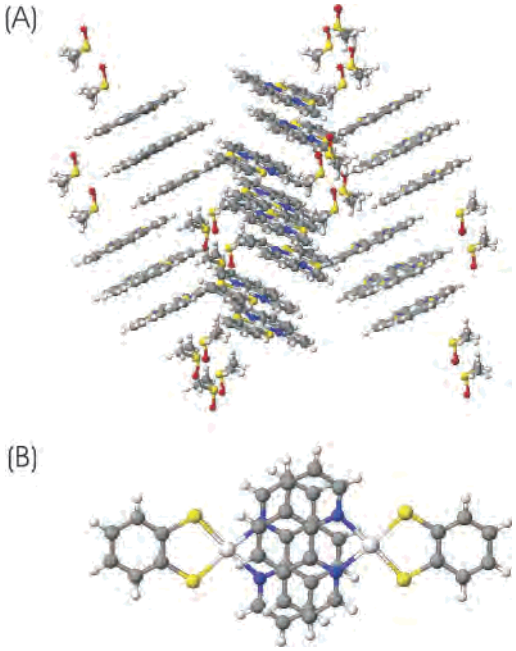

Figure 2. (A) Crystal packing in **1**. (B) View of two molecules packing in **1**.

in a V type assembly. In each column the individual molecules are stacked in a head-to-tail arrangement (the representative Pd molecules are shown in Figure 2B). For **1**·dmso molecules are positioned so that the metal center of one molecule is situated directly above a bridging carbon on the 1,10-phenanthroline ring of an adjacent molecule. The intermolecular distances between the stacks of **1** are 3.36(1) Å, while the closest Pd···Pd separation between neutral complex chains is 68.64(8) Å, which is significantly larger than the Pt···Pt separation in a chain (∼3.3−3.7 Å). The head-to-tail arrangement is reversed to a head-to-head one since a dmso molecule is sandwiched between two complex molecules. From these data we conclude that no strong Pd···Pd interactions are present in the molecules in their crystalline form, and the only possible intermolecular interaction is that of π stacking, whose nature can be changed by the involvement of a solvent molecule, in contradiction to Pt analogous complexes where both Pt···Pt and π interactions are present, without changing the head-to-tail arrangement.[23b,c] This will be further discussed in the emission spectroscopy section.

Complexes **1**−**5** exhibit significant differences in their optical and electronic properties. The most obvious ones are in their color. Crystalline and solution samples of **1** and **2**

Table 3. Comparison of Calculated Selected Bond Lengths (Å) and Angles (deg) for **1**−**5** with Experimental Values from X-ray Analysis

	1		**2**[7a]		**3**[7b]		**4**	**5**[11]	
	exptl	calcd	exptl	calcd	exptl	calcd	calcd	exptl	calcd
M−N[a]	2.096(8)	2.128	2.071(2)	2.120	2.050(5)	2.095	2.099	2.049(4)	2.092
M−S[a]	2.261(3)	2.283	2.245(1)	2.286	2.248(2)	2.299	2.296	2.250(1)	2.302
C−S	1.787(10)	1.775	1.762(2)	1.774	1.761(6)	1.771	1.759	1.743(7)	1.754
C═N	1.368(12)	1.364	1.353(3)	1.358	1.367(8)	1.363	1.362	1.362(7)	1.365
$C{=}C^{dithiol.}$	1.376(13)	1.401	1.396(3)	1.401	1.373(8)	1.402	1.365	1.346(14)	1.341
$C{=}C^{diim.}$	1.437(13)	1.434	1.474(3)	1.476	1.464(8)	1.466	1.469	1.469(10)	1.462
$\varphi_{diim.}$	80.2(3)	78.69	79.41(6)	77.85	80.1(2)	78.00	78.04	79.26(16)	78.10
$\varphi_{dithiol.}$	89.17(10)	88.49	88.67(2)	88.16	89.0(1)	88.26	88.44	88.67(6)	88.05

[a] The average value of both distances.

Table 4. UV−Vis and Emission Data for **1**−**5**

complex	λ_{max}[a]	E_{max}[b]	E_{max}[c]	ΔE[d]	λ_{em}[e] (E_{max})
1	531 (3200)	2.33	2.10	1.40	
	388 (1400)	3.20		3.40	
	359 (1600)	3.45		3.50	
	321 (3400)	3.86			
	295 (31000)	4.20			
2	524 (2850)	2.37	2.13	1.42	
	361 (1400)	3.43		3.43	
	308 (21000)				
3	602 (6000)	2.06	1.85	1.53	690 (1.80)
	365 (1900)	3.40		3.41	
	314 (23000)	3.95			
4	453 (4320)	2.74	2.48	1.68	632 (1.96)
	318 (8700)	3.90		3.82	
5	613 (4500)	2.02	1.78	1.48	712 (1.74)
	330sh	3.76		3.67	
	304 (18600)	4.05			

[a] Absorption maxima in $CHCl_3$ in nm (molar extinction coefficient in M^{-1} cm^{-1}). [b] Absorption maxima in $CHCl_3$ in eV. [c] Absorption maximum for the main band in C_6H_6 in eV. [d] TDDFT calculated transition energy, given in eV. [e] Emission maxima in DMM in nm (eV).

are dark red, whereas **4** is brown red and **5** gives deep-purple solid and solutions. Consistent with this observation, the intense charge-transfer absorption band that gives rise to the color of these complexes is both blue-shifted and broadened for **1** and **2** as compared to **3** and **5**. Moreover the Pd(diimine)(dithiolate) complexes in contradiction to Pt ones do not luminescence as has been indicated both from our experimental results and the literature[2k−l,7b] (Table 4).

In an effort to better understand the widely differing behavior of these two closely related groups of complexes (Pd and Pt ones) and consequently the role of the metal atom, diimine, and the "noninnocent" dithiolene ligand[23] in their electronic structure, a study of the latter one of **1**−**5** has been performed by means of DFT formalism. The DFT-calculated bond lengths and angles fit well with the experimentally obtained ones for **1**−**5** (Table 3).

2.2. Absorption Spectroscopy and Calculations. All M(diimine)(dithiolate) complexes exhibit broad and partially structured long-wavelength absorption bands (Figure 3 and Table 4). These bands show negative solvatochromism, indicating their charge-transfer character. The latter one has been assigned as LL′CT by Vogler[4i] and later by Srivastava,[4b] as MMLL′CT by Eisenberg and co-workers[2k,q] after their fundamental work while recently the general term "charge transfer-to-diimine" has been employed.[2g,i] Moreover, Eisenberg *et al.*, studying a series of compounds, attributed the presence of this solvatochromic band to the existence of a π^*-conjugated system on the N-donor ligand; the latter one is not necessary for the S-donor ligand. This observation supports the assignment of HOMO and LUMO orbitals based on electrochemical data.[2n] Later they gave more insight on the structural dependence of the electronic and nonlinear optical properties of this type of complex and revealed the way of tuning them.[2f,g,i]

Complexes **1**−**5** are representative for the family of M(diimine)(dithiolate) complexes, providing us with the necessary data to switch between the metals, diimines, and dithiolate ligands. While absorption and emission spectra for some of the complexes have been reported previously, we

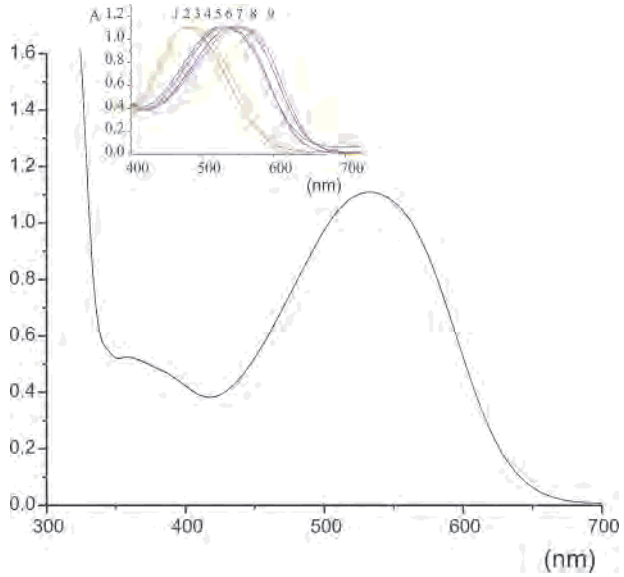

Figure 3. UV−vis spectra of **1** in chloroform. Inset: the low energy band of **1** in common solvents (1 = acetonitrile, 2 = dmso, 3 = dmf, 4 = 1,2-dme, 5 = dibromomethane, 6 = chloroform, 7 = THF, 8 = 1,4-dioxane, 9 = benzene). Absorbance maxima have been normalized for illustrative purposes.

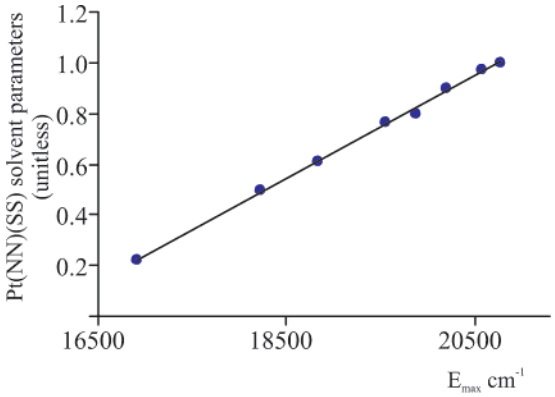

Figure 4. Linear correlation between Pt(NN)(SS) solvent parameters and observed (E_{max}) low-energy absorption (R^2 = 0.99).

chose to reexamine their behavior in order to ensure that all measurements were performed under standard conditions. Figure 4 shows the absorption spectrum of **1** in chloroform, as a representative example of the whole series of complexes. A total shift of about 1931 cm^{-1} (83 nm) is observed from dibromomethane to acetonitrile, and if we identity benzene in our analysis (the complexes' solubility is very low in it), the blue-shift expands to 3875 cm^{-1} (110 nm) (inset Figure 3).

The transition energy $E_{MMLL'CT}$ has been correlated to various empirical solvent parameters and experimentally derived constants.[25] Linear coefficient is quite satisfactory both in the correlation of $E_{MMLL'CT}$ with Reichard's[25c] E_T parameters (R = 0.98) and with the empirical solvent scale introduced by Cummings and Eisenberg[2i] (R = 0.99) (Figure 4); the latter one is based on the results for Pt(dbbpy)(tdt) in order to determine the relative degree of solvatochromism of related complexes.[2i]

In order to assign the absorption bands, and in particular to determine the metal and dithiolate ligand contributions to

Table 5. G98/B3LYP Calculated One Electron Energies and Percentage Composition of Selected Frontier MOs of **1**−**5**, Expressed in Terms of Composing Fragments[a]

MO	E_{eV}	diimine	dithiol.	metal	MO	E_{eV}	diimine	dithiol.	metal
		1					**4**		
		Unoccupied					Unoccupied		
$9a_2$	−0.90	99.5	0.0	0.5	$9a_2$	−1.60	3.8	94.4	1.8
$12b_1$	−1.56	99.0	0.3	0.8	$33b_2$	−1.89	10.0	46.1	43.9
$35b_2$	−1.69	11.8	46.6	41.7	$8a_2$	−2.37	96.5	2.5	0.9
$8a_2$	−2.73	99.3	0.2	0.5	$11b_1$	−2.59	98.3	0.4	1.2
$11b_1$	**−2.89**	**92.8**	**4.3**	**2.9**	**$10b_1$**	**−3.49**	**90.4**	**5.0**	**4.5**
		Occupied					Occupied		
$10b_1$	**−4.66**	**5.4**	**85.6**	**9.0**	**$9b_1$**	**−5.51**	**7.5**	**81.1**	**11.4**
$7a_2$	−5.11	0.9	88.8	10.3	$7a_2$	−6.53	2.8	67.0	30.2
$41a_1$	−6.25	2.8	33.9	63.4	$37a_1$	−7.15	7.8	21.0	71.2
$6a_2$	−6.72	1.7	75.9	22.3	$8b_1$	−7.63	7.9	49.3	42.8
$9b_1$	−6.84	9.1	52.7	38.1	$36a_1$	−8.17	2.0	52.3	45.7
$40a_1$	−7.22	4.7	48.3	47.0	$32b_2$	−8.20	18.4	61.2	20.3
		2					**5**		
		Unoccupied					Unoccupied		
$39a_1$	−0.67	65.7	−9.4	43.7	$33a_1$	−0.58	57.1	4.6	38.4
$33b_2$	−1.71	9.2	48.2	42.6	$28b_2$	−1.01	12.6	44.9	42.4
$8a_2$	−1.79	99.0	0.2	0.8	$7a_2$	−1.69	98.4	0.4	1.3
$11b_1$	−2.08	99.0	0.3	0.8	$10b_1$	−1.92	98.1	0.5	1.4
$10b_1$	**−2.93**	**92.4**	**4.6**	**3.0**	**$9b_1$**	**−2.81**	**84.6**	**9.7**	**5.6**
		Occupied					Occupied		
$9b_1$	**−4.69**	**5.8**	**85.4**	**8.8**	**$8b_1$**	**−4.50**	**12.7**	**78.0**	**9.3**
$7a_2$	−5.14	0.8	89.1	10.1	$6a_2$	−5.68	3.0	67.4	29.6
$38a_1$	−6.28	8.6	39.0	52.3	$32a_1$	−6.35	7.7	23.9	68.4
$6a_2$	−6.75	1.8	75.9	22.3	$7b_1$	−7.04	11.6	25.8	62.6
$8b_1$	−6.89	5.0	55.6	39.4	$31a_1$	−7.26	4.3	52.9	42.8
$32b_2$	−7.22	18.1	60.8	21.1	$27b_2$	−7.36	17.6	62.2	20.1
		3							
		Unoccupied							
$39a_1$	−0.66	59.9	2.3	37.8					
$33b_2$	−1.06	6.5	46.6	46.9					
$8a_2$	−1.8	98.2	0.5	1.3					
$11b_1$	−2.04	98.1	0.5	1.4					
$10b_1$	**−2.92**	**87.4**	**7.2**	**5.4**					
		Occupied							
$9b_1$	**−4.63**	**10.0**	**79.9**	**10.0**					
$7a_2$	−5.13	1.7	83.7	14.6					
$38a_1$	−6.4	6.7	24.2	69.1					
$6a_2$	−6.73	3.3	70.0	26.7					
$8b_1$	−6.82	7.6	51.9	40.5					
$37a_1$	−7.27	3.4	53.1	43.5					

[a] HOMO and LUMO orbitals are shown in bold.

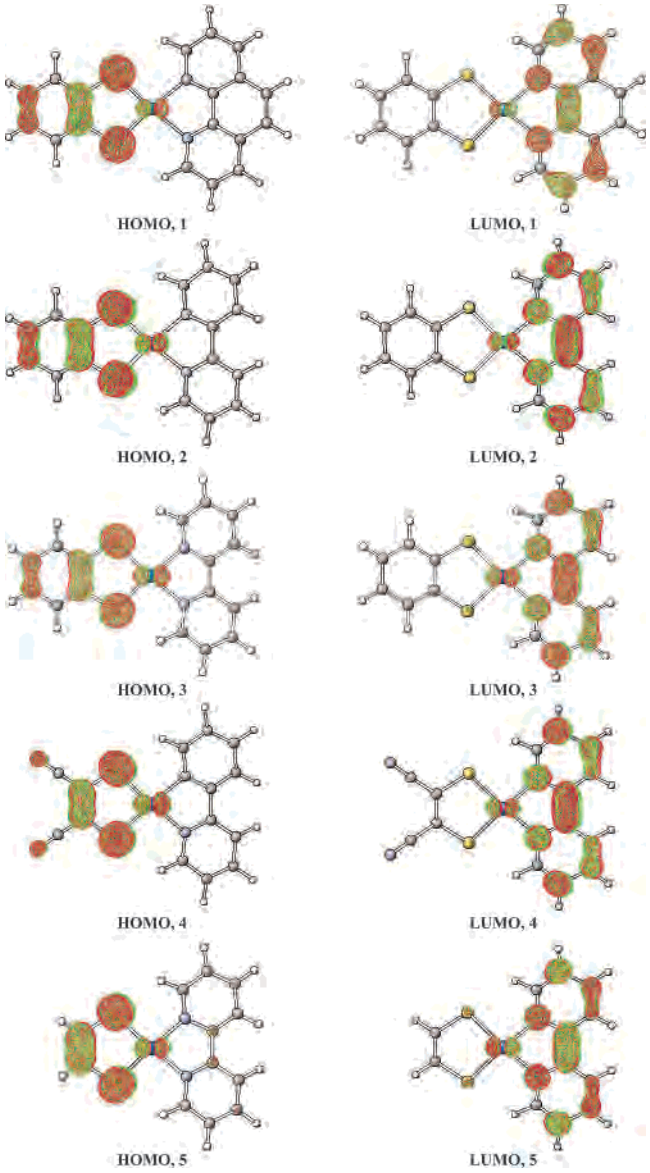

Figure 5. 0.05 au contour plots of HOMOs and LUMOs of **1**−**5**.

the highest occupied MOs (HOMO), DFT calculations were performed on all five complexes (**1**−**5**) based on crystallographic data (Table 3). The orbital energies along with the contributions from the two ligands and the metal are given in Table 5. In all five complexes the five highest occupied orbitals are denoted mainly dithiolate/metal in character with the major contribution being on HOMO−1 and HOMO orbitals, while no pure d_{metal} orbitals have been observed due to the noninnocent nature of the dithiolate ligand. In other words, the HOMO, a b_1 orbital, is composed mainly of sulfur $3p_z$ orbitals that form antibonding interactions with metal d_{xz} orbitals and carbon $2p_z$ orbitals on the chelating ring (Figure 5). The high contribution of $3p_z$ on the HOMO orbital is probably the reason that these complexes are easily oxidized to give sulfinated and sulfonated derivatives as has been reported before.[4a,7a]

Although the LUMO is calculated to be almost exclusively located on diimine, a limited contribution of metal and dithiolate ligand still exists. More precisely, apart from the interactions between carbon atoms of the carbohydrated core, antibonding interactions of the $2p_z$ nitrogen orbitals with the d_{xz} metal orbital are also present. The aforementioned pattern, consistent with π*-back-bonding theory, indicates that electron back-donation to phen or bpy is reduced by the presence of dithiolate as compared with other diimine complexes.[27a]

Moreover LUMO orbitals having b_1 and a_2 symmetry for phen and b_1 for bpy are characteristic for the diimine moiety, and they are the optically active orbitals as TDDFT calculations indicated, in agreement with the references on the phen and bpy complexes.[8c,9a,27b]

Finally, the first b_2 orbital (LUMO+2 for **1** and LUMO+3 for the rest) is formed by the contributions from all fragments with the major ones coming from both the metal and the dithiolate (Table 5). Our DFT calculations indicate that the HOMO is localized mainly on the dithiolate, admixed with

(27) (a) Vlček, A., Jr. *Coord. Chem. Rev.* **2002**, *230*, 225−242. (b) Ernst, S.; Vogler, C.; Klein, A.; Kaim, W. *Inorg. Chem.* **1996**, *35*, 1295−1300.

metal, and the LUMO almost exclusively on the diimine. For **1** and **2** LUMOs, as already has been indicated, are characteristic for the two diimines, whereas valence occupied orbitals exhibit the same character due to the identity of the dithiolate and the metal. As from the energetics view phen and bpy show almost identical π*-accepting ability (Table 5), it is expected that the HOMO−LUMO gap of these complexes will be very close in energy, assuming identical solvation energy differences for the two levels, in accordance with the experimental results (λ_{max} = 531 nm for **1** and λ_{max} = 524 nm for **2** in $CHCl_3$).

The role of the nature of the dithiolate in the electronic structure of the M(diimine)(dithiolate) complexes is examined in complexes **3**−**5**, by choosing substituents with different π*-accepting ability. More precisely, −CN is a good π*-accepting group as compared to −H, whereas benzenedithiolate is a widely used aromatic ligand. From earlier experimental work,[1−5] it is anticipated that electron accepting groups stabilize the HOMO, leaving the LUMO quite unaffected. Our DFT results support the first trend, and the HOMO is stabilized in the order mnt^{2-} > bdt^{2-} > edt^{2-}, but the LUMO is also stabilized in the same order. Moreover the participation of both metal and dithiolate orbitals in the latter is enhanced in the reversed order in compliance with π*-back-bonding theory. Both trends enlarge the HOMO−LUMO gap (2.03 eV for **4** to 1.71 eV for **3** and 1.69 eV for **5**), in accordance with the observed UV−vis spectra. Furthermore, the influence of a −CN substituent can be denoted by the low lying orbital (LUMO+4) of **4**, which is almost entirely localized on the mnt^{2-} ligand instead of the diimine, which is the case for the other four complexes. As derived from our results, the $9a_2$ orbital plays a very important role to the emission characteristics of M(diimine)(dithiolate) complexes.

Comparing **2** to **3** a few amendments should be incorporated in the previous model, when the discussion comes to the metal. First of all, metal's contribution is increased both in occupied (HOMO, 10.0% for **3** compared to 8.8% for **2)** and virtual orbitals (LUMO, 3.0% for **2** and 5.4% for **3**). This trend is attributed to the better metal−ligand overlap induced by the 5d-orbitals of Pt compared to 4d-orbitals of Pd. Moreover the reduction of the HOMO−LUMO gap by the engagement of Pt (1.76 eV for **2** and 1.71 eV for **3**) explains the redox behavior of two complexes[7a] and reinforces at the same time the mixed-metal-ligand-to-ligand notation for the observed charge-transfer band.

The solvent effect modeled by the PCM (polarizable continuum model) procedure affects mainly the composition of HOMOs with large Pd contributions. When the solvent effect is introduced (i.e. acetonitrile), the Pd contributions within **1** enlarge to 10.9%, 12.2%, 67.2%, and 29.0% in orbitals $10b_1$, $7a_2$, $41a_1$, and $6a_2$, respectively. In addition, HOMO−1 to HOMO−4 orbitals exhibit larger dithiolate and less diimine character and the HOMO−LUMO separation increases. The LUMO character, on the other hand, even if it does not change substantially, has more diimine character (in acetonitrile there is 96% phen character in the $11b_1$ orbital). The model of solvation (PCM in G98) enlarges the HOMO−LUMO separation by 0.37 to 0.67 eV shifting from benzene to acetonitrile and affects the frontier orbitals comparably.

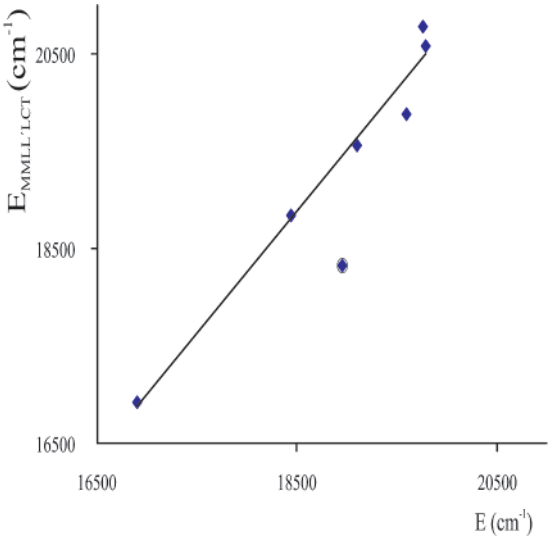

Figure 6. Linear correlation between experimental ($E_{MMLL'CT}$) and the HOMO−LUMO energy gap (ΔE) calculated by DFT (R^2 = 0.98). From left to right: acetonitrile, dmso, acetone, dichloromethane, acetonitrile, thf, and acetonitrile. THF is not included in the regression analysis.

Although Koopmans' theorem does not apply to DFT and the energies of Kohn−Sham orbitals cannot be used as in the case of Hartree−Fock calculations, it is widely accepted that the energy difference ΔE between the HOMO and the LUMO can be considered as a valuable parameter.[26] Based on that assumption, we tested the applicability of the PCM[27] to this hardly electronically describable inorganic complex, by checking the relationship $E_{MMLL'CT} = f(\Delta E)$ (Figure 6) for seven solvents, namely, acetonitrile, DMSO, acetone, dichloromethane, chloroform, tetrahydrofuran, and benzene. As it is denoted in Figure 6, the correlation is perfect especially in the case of nonpolar solvents, which is pretty reasonable, due to the large transition dipole moments that escort these complexes. THF is an exception. As we cannot explain this inconsistency by the aid of experimental aspects, we assume that it is due to the specific parametrization of THF as it is implemented on the polarizable continuum model. Otherwise the poor correlation of THF could be a consequence of specific solvation interactions of THF molecules with the Pt center or S atoms. But experimental evidence for this does not exist.

The above-mentioned expectations are supported by time dependent (TD) DFT calculations. Selected low lying singlet and triplet excited states together with their vertical excitation energies and oscillator strengths for **1**, **2**, **3**, **4**, and **5** are displayed in Tables 6, 7, 8, 9, and 10, respectively. The transitions under study fulfill the criteria posed by Casida.[28] The TDDFT calculated lowest transitions of all five complexes can be described as having mainly mixed metal/dithiolate to diimine (MMLL′CT) character in agreement with the "classical" assignment. In particular the lowest broad

(28) Casida, M. E.; Jamorski, C.; Casida, K. C.; Salahub, D. R. *J. Chem. Phys.* **1998**, *108*, 4439−4449.

Table 6. Selected TDDFT Calculated Energies and Compositions of the Lowest Lying Singlet and Triplet Energy States Together with Oscillator Strengths of **1**[a]

state	composition[b]	ΔE[c]	f[d]	character
		Singlets		
b^1A_1	**$10b_1$(HOMO) → $11b_1$(LUMO), 82% $7a_2$(HOMO−1) → $8a_2$(LUMO+1), 4%**	**1.40**	**0.0962**	**bdt/Pd → phen (MMLL′CT)**
a^1B_2	$10b_1$(HOMO) → $8a_2$(LUMO+1), 95%	1.43	0.0044	bdt/Pd → phen (MMLL′CT)
e^1A_1	$9b_1$(HOMO−4) → $11b_1$(LUMO), 76% $6a_2$(HOMO−3) → $8a_2$(LUMO+1), 17%	3.40	0.0234	bdt/Pd → phen (MMLL′CT)
f^1A_1	$6a_2$(HOMO−3) → $8a_2$(LUMO+1), 79% $9b_1$(HOMO−4) → $11b_1$(LUMO), 16%	3.50	0.0276	bdt/Pd → phen (MMLL′CT)
		Triplets		
a^3A_1	$10b_1$(HOMO) → $11b_1$(LUMO), 100%	1.09		bdt/Pd → phen (MMLL′CT)
a^3B_2	$10b_1$(HOMO) → $8a_2$(LUMO+1), 100%	1.35		bdt/Pd → phen (MMLL′CT)
b^3B_2	$7a_2$(HOMO−1) → $11b_1$(LUMO), 100%	1.58		bdt/Pd → phen (MMLL′CT)
a^3A_2	$10b_1$(HOMO) → $35b_2$(LUMO+2), 100%	1.65		bdt/Pd → bdt/Pd (LMCT)
b^3A_1	$7a_2$(HOMO−1) → $8a_2$(LUMO+1), 100%	1.86		bdt/Pd → phen (MMLL′CT)

[a] The principal singlet transition responsible for the main absorption band in the vis is shown in bold. [b] Compositions of electronic transitions are expressed in terms of contributing excitations between ground-state Kohn−Sham molecular orbitals. [c] Transition energy from the a^1A_1 ground state in eV. [d] Oscillator strength.

Table 7. Selected TDDFT Calculated Energies and Compositions of the Lowest Lying Singlet and Triplet Energy States Together with Oscillator Strengths of **2**[a]

state	composition[b]	ΔE[c]	f[d]	character
		Singlets		
b^1A_1	**$9b_1$(HOMO) → $10b_1$(LUMO), 83%**	**1.42**	**0.1091**	**bdt/Pd → bpy (MMLL′CT)**
a^1B_2	$7a_2$(HOMO−1) → $10b_1$(LUMO), 95%	1.66	0.0017	bdt/Pd → bpy (MMLL′CT)
e^1A_1	$8b_1$(HOMO−4) → $10b_1$(LUMO), 92%	3.43	0.0383	bdt/Pd → bpy (MMLL′CT)
e^1B_1	$9b_1$(HOMO) → $39a_1$(LUMO+4)	3.60	0.0040	bdt/Pd → bpy/Pd (LMCT/LLCT)
		Triplets		
a^3A_1	$9b_1$(HOMO) → $10b_1$(LUMO), 100%	1.06		bdt/Pd → bpy (MMLL′CT)
a^3B_2	$7a_2$(HOMO−1) → $10b_1$(LUMO), 100%	1.57		bdt/Pd → bpy (MMLL′CT)
a^3A_2	$9b_1$(HOMO) → $33b_2$(LUMO+3), 94% $8b_1$(HOMO−4) → $33b_2$(LUMO+3), 5%	1.66		bdt/Pd → bdt/Pd (LMCT)
a^3B_1	$7a_2$(HOMO−1) → $33b_2$(LUMO+3), 97% $6a_2$(HOMO−3) → $33b_2$(LUMO+3), 3%	1.94		bdt/Pd → bdt/Pd (LMCT)
b^3A_1	$9b_1$(HOMO) → $11b_1$(LUMO+1), 100%	2.00		bdt/Pd → bpy (MMLL′CT)

[a] The principal singlet transition responsible for the main absorption band in the vis is shown in bold. [b] Compositions of electronic transitions are expressed in terms of contributing excitations between ground-state Kohn−Sham molecular orbitals. [c] Transition energy from the a^1A_1 ground state in eV. [d] Oscillator strength

Table 8. Selected TDDFT Calculated Energies and Compositions of the Lowest Lying Singlet and Triplet Energy States Together with Oscillator Strengths of **3**[a]

state	composition[b]	ΔE[c]	f[d]	character
		Singlets		
b^1A_1	**$9b_1$(HOMO) → $10b_1$(LUMO), 78%**	**1.53**	**0.1501**	**bdt/Pt → bpy (MMLL′CT)**
a^1B_2	$7a_2$(HOMO−1) → $10b_1$(LUMO), 93%	1.64	0.0035	bdt/Pt → bpy (MMLL′CT)
e^1A_1	$8b_1$(HOMO−4) → $10b_1$(LUMO), 89%	3.41	0.0413	bdt/Pt → bpy (MMLL′CT)
e^1B_1	$9b_1$(HOMO) → $39a_1$(LUMO+4), 98%	3.64	0.0036	bdt/Pt → bpy/Pt (LMCT/LLCT)
e^1B_2	$9b_1$(HOMO) → $9a_2$(LUMO+5), 96%	3.68	0.0186	bdt/Pt → bpy (MMLL′CT)
f^1B_2	$38a_1$(HOMO−2) → $33b_2$(LUMO+3), 86%	3.85	0.0019	Pt/bdt → Pt/bdt (LF)
		Triplets		
a^3A_1	$9b_1$(HOMO) → $10b_1$(LUMO), 100%	1.00		bdt/Pt → bpy (MMLL′CT)
a^3B_2	$7a_2$(HOMO−1) → $10b_1$(LUMO), 100%	1.47		bdt/Pt → bpy (MMLL′CT)
b^3A_1	**$9b_1$(HOMO) → $11b_1$(LUMO+1), 100%**	**2.02**		**bdt/Pt → bpy (MMLL′CT)**
b^3B_2	$9b_1$(HOMO) → $8a_2$(LUMO+2), 100%	2.23		bdt/Pt → bpy (MMLL′CT)

[a] The principal singlet and triplet transitions responsible for the main absorption and emission bands in the visible region are shown in bold. [b] Compositions of electronic transitions are expressed in terms of contributing excitations between ground-state Kohn−Sham molecular orbitals. [c] Transition energy from the a^1A_1 ground state in eV. [d] Oscillator strength.

absorption band for complexes **1**−**5**, characterized by strong negative solvatochromism, can be assigned to an a^1A_1 → b^1A_1 transition, which is described mainly as a HOMO → LUMO in full agreement to what is experimentally derived for complexes of this type.[2g,i] A referee argued that since the HOMO has about 80% dithiol and LUMO 90% diimine character with approximately equal amounts of metal for both Pd and Pt complexes (considering the difference of a few percent for both metals not significant) (Table 5), then, analogously to the $Ru(bpy)_3^{2+}$, the visible transition is best described as a dithiolate to diimine (LL′CT) transition. This statement cannot be ignored especially if someone takes under consideration the values of the percentage of HOMO and LUMO very strictly. Actually, that was our very first conclusion. However, this approach could not explain the differences in chemistry for the (diimine)(dithiolate) com-

Table 9. Selected TDDFT Calculated Energies and Compositions of the Lowest Lying Singlet and Triplet Energy States Together with Oscillator Strengths of **4**[a]

state	composition[b]	ΔE[c]	f[d]	character
	Singlets			
b^1A_1	**$9b_1$(HOMO) → $10b_1$(LUMO), 83%**	**1.68**	**0.1229**	**mnt/Pt → bpy (MMLL′CT)**
a^1B_2	$7a_2$(HOMO−1) → $10b_1$(LUMO), 95%	2.36	0.0008	mnt/Pt → bpy (MMLL′CT)
e^1A_1	$8b_1$(HOMO−3) → $10b_1$(LUMO), 49% $7a_2$(HOMO−1) → $8a_2$(LUMO+2), 42%	3.66	0.1355	mnt/Pt → bpy (MMLL′CT)
e^1B_2	$37a_1$(HOMO−2) → $33b_2$(LUMO+3), 63% $9b_1$(HOMO) → $9a_2$(LUMO+4), 13% $9b_1$(HOMO) → $10a_2$(LUMO+5), 9%	3.82	0.0375	Pt/mnt → mnt/Pt (MLCT)
	Triplets			
a^3A_1	$9b_1$(HOMO) → $10b_1$(LUMO), 100%	1.25		mnt/Pt → bpy (MMLL′CT)
a^3B_2	$7a_2$(HOMO−1) → $10b_1$(LUMO), 97%	2.20		mnt/Pt → bpy (MMLL′CT)
b^3B_2	**$9b_1$(HOMO) → $9a_2$(LUMO+4), 67%** **$9b_1$(HOMO) → $8a_2$(LUMO+2), 28%** **$8b_1$(HOMO−3) → $9a_2$(LUMO+4), 7%**	**2.22**		**mnt/Pt → mnt (MLCT)** **mnt/Pt → bpy (MMLL′CT)** **mnt/Pt → mnt (MLCT)**
b^3A_1	$9b_1$(HOMO) → $11b_1$(LUMO+1), 100%	2.25		mnt/Pt → bpy (MMLL′CT)
a^3A_2	$9b_1$(HOMO) → $33b_2$(LUMO+3), 100%	2.31		mnt/Pt → mnt/Pt (LMCT)

[a] The principal singlet and triplet transitions responsible for the main absorption and emission bands in the visible region are shown in bold. [b] Compositions of electronic transitions are expressed in terms of contributing excitations between ground-state Kohn−Sham molecular orbitals. [c] Transition energy from the a^1A_1 ground state in eV. [d] Oscillator strength.

Table 10. Selected TDDFT Calculated Energies and Compositions of the Lowest Lying Singlet and Triplet Energy States Together with Oscillator Strengths of **5**[a]

state	composition[b]	ΔE[c]	f[d]	character
	Singlets			
b^1A_1	**$8b_1$(HOMO) → $9b_1$(LUMO), 71%**	**1.48**	**0.1284**	**edt/bpy/Pt → bpy (MMLL′CT)**
c^1A_1	$8b_1$(HOMO) → $10b_1$(LUMO+1), 97%	2.00	0.0067	edt/bpy/Pt → bpy (MMLL′CT)
d^1B_2	$8b_1$(HOMO) → $7a_2$(LUMO+5), 94%	3.57	0.0276	edt/bpy/Pt → bpy (MMLL′CT)
e^1A_1	$7b_1$(HOMO−3) → $9b_1$(LUMO), 77% $6a_2$(HOMO−1) → $7a_2$(LUMO+2), 11%	3.67	0.0634	Pt/edt/bpy → bpy (MLCT)
	Triplets			
a^3A_1	$8b_1$(HOMO) → $9b_1$(LUMO), 100%	0.79		edt/bpy/Pt → bpy (MMLL′CT)
b^3A_1	$8b_1$(HOMO) → $10b_1$(LUMO+1), 100%	1.88		edt/bpy/Pt → bpy (MMLL′CT)
a^3B_2	**$6a_2$(HOMO−1) → $9b_1$(LUMO), 95%** **$8b_1$(HOMO) → $7a_2$(LUMO+2), 3%**	**1.94**		**edt/Pt → bpy (MMLL′CT)**
b^3B_2	$8b_1$(HOMO) → $7a_2$(LUMO+2), 94% $6a_2$(HOMO−1) → $9b_1$(LUMO), 6% $6a_2$(HOMO−1) → $7a_2$(LUMO+2), 12%	2.09		edt/bpy/Pt → bpy (MMLL′CT) edt/Pt → bpy (MMLL′CT)

[a] The principal singlet and triplet transitions responsible for the main absorption and emission bands in the visible region are shown in bold. [b] Compositions of electronic transitions are expressed in terms of contributing excitations between ground-state Kohn−Sham molecular orbitals. [c] Transition energy from the a^1A_1 ground state in eV. [d] Oscillator strength.

plexes with the same ligands but different metals (photooxidation, photoluminescence, etc.) For us the role of the metal is not just "the right connector between two conductors"; we judge that its partial is much more significant than this. A closer inspection of Tables 6−10 revealed that the main transition HOMO → LUMO consists of only 71−83% of the lowest broad absorption band for complexes **1**−**5** in contradiction to $Ru(bpy)_3^{2+}$ and other complexes,[8f,20b] where the main transition assigned to MLCT is over 90−98%. In other words, in the case of (diimine)(dithiolate) complexes a percentage 17−29% consists of transitions from lower HOMOs than the frontier, to LUMOs. In Table 5 it is clear that the metal contribution in HOMO−1,2,3,4, for all five complexes, is substantially greater than its contribution to the HOMO. So although the participation of each one of these transitions is not larger than 2% in the lowest broad absorption band, their overall contribution indicates a significant electron transfer from the metal to the diimine. In this context, the metal percentage difference may be considered as significant and the main transition must be assigned as MMLL′CT.

The calculated energies agree only moderately with the experimental ones[29] (Table 4). One reason is the strong solvatochromism of the compounds, as displayed by the shift of the experimental energies going from chloroform to benzene as solvent. However, they agree at least qualitatively, showing a number of low energy transitions of weak to moderate intensity which contributes to the broadness of the band in the range of 450−700 nm together with their character in the spectra. The calculated (by TDDFT) E_{max} of **3** is greater than **2** in contradiction to experimental data. This discrepancy must be due to factors that were not taken into account in the TDDFT calculations, such as spin−orbit coupling due to the platinum atom (these calculations are not supported from the G98 version of the Gaussian program) and which would diminish the energy about 0.3 eV, the influence of vibrational motion of the molecule which can increase orbital overlap (and as a consequence the increase of oscillator strength), electronic through-solvent interaction, and so on. However, in view of the transition energies in

(29) Fantacci, S.; De Angelis, F.; Selloni, A. *J. Am. Chem. Soc.* **2003**, *125*, 4381−4387.

the same metal complexes, we feel confident that our present assignment of the observed absorption bands to these calculated transitions is the correct one.

All the aforementioned complexes have a second set of absorption bands at 350−400 nm which are less intense than the previous one. For example in the case of **1**, two weak bands or more precisely shoulders are observed in all solvents around 360 nm (359 and 388 nm in chloroform). These bands are precisely predicted by TDDFT calculations and are assigned to $a^1A_1 \rightarrow e^1A_1$ and $a^1A \rightarrow f^1A_1$ transitions. Both of them have $9b_1 \rightarrow 11b_1$ (HOMO−4 → LUMO) and $6a_2 \rightarrow 8a_2$ (HOMO−3 → LUMO+1) character with approximately reversed weights (Table 6). In view of the character of the orbitals involved, it can be best described as mixed metal/ligand to ligand transition. The solvent independence of these bands is reflected by the fact that both $6a_2$ and $9b_1$ orbitals are mainly localized on sulfur atoms and at the same time the contribution from the metal d orbitals is relatively high diminishing $\Delta\mu_{ge}$ and hence the ΔE_{solv} of the involved states. Moreover, our TDDFT calculations support previous experimental results[2g] indicating that the opposite charge-transfer transition diimine → dithiolate is very high in energy and it is not observed to the UV−vis region of the spectrum.

The low lying transition within **2** has similar character as in **1**, assigned to the HOMO ($9b_1$) → LUMO ($10b_1$) transition, while the moderate solvatochromic band is observed at 3.43 eV in full agreement with the experiment (3.44 in THF). This transition is also HOMO−4 ($8b_1$) → LUMO ($10b_1$) in character, while no other transition with comparable energy is observed (as in **1**) due to the absence of an a_2 orbital (LUMO+1) in the bpy ligand (Table 7).

Proceeding in a similar way, the lowest-energy absorprtion band is assigned to a HOMO → LUMO transition with 78% $9b_1 \rightarrow 10b_1$ for **3**, 71% $8b_1 \rightarrow 9b_1$ for **4**, and 83% $9b_1 \rightarrow 10b_1$ for **5**, whereas the higher energy absorption (350−400 nm) is assigned to a HOMO−4 → LUMO transition with 89% $8b_1 \rightarrow 10b_1$ for **3** (Table 8), while for **4** and **5**, it is attributed to HOMO−3 → LUMO (with 49% and 77% contribution, respectively) and HOMO−1 → LUMO+2 (with 42% and 11%, respectively) (Tables 9 and 10).

Comparing **1**, **2**, **3**, **4**, and **5** we may notice that platinum complexes exhibit higher oscillator strength than the palladium ones (Tables 6−10), in accordance with the molar extinction coefficient (Table 4). This trend could indicate the higher participation of the metal to charge transfer procedure due to the greater extent of occupied space of the metal d-orbitals, which results in an extensive π-delocalization in the case of Pt complexes. The latter is reflected in the higher percentage of metal d-orbitals in HOMOs for Pt complexes (Table 5). The metal increases both the wavelength and molar extinction coefficient of the MML to diimine absorption band following the order Pd(II) < Pt(II) (Table 4, **2** vs **3**). This observation strongly supports metal orbital involvement in the charge-transfer to diimine excited state.

It may also be observed that HOMO's dithiolate and LUMO's diimine character is increased in the series $mnt^{2-} > bdt^{2-} > edt^{2-}$, Pd > Pt and phen ∼ bpy. In the reversed order is increased HOMO's diimine and LUMO's dithiolate character. In other words, if the electron donating ability on the dithiolate or electron accepting ability on the diimine is increased, by tuning the ligand substituents' structure appropriately, then the HOMO−LUMO gap is reduced, increasing at the same time the orbital mixing. This delocalization provides a less strict assignment to the observed transition.

Finally, since M(diimine)(dithiolate) compounds are probable candidates for materials with enhanced NLO properties (charge-transfer excited states are the origin of nonlinearity), a comment should be made based on theoretical calculations. According to a simplified version of the two-state model, the intrinsic hyperpolarizabilty is given by the relation[30]

$$\beta_0 = 1.617\lambda_{max}{}^3 f \Delta\mu_{ge}$$

and β_0 depends on λ_{max},[3] oscillator strength, and difference in dipole moment between excited and ground state. Alternatively according to the two-state model,[31] a smaller energy gap for the charge-transfer transition should result in a larger β value. Modification of both bipyridine ligand and dithiolate/metal is an effective method of lowering the π*-acceptor orbital or increasing the π*/d-donor orbital, respectively and thus reducing the energy gap for the charge-transfer transition. Probable candidates would be diimines with extended π*-conjugated systems or diimines carrying electron accepting groups and dithiolates with π*-donor groups as substituents. This trend can be rationalized, since the use of a strong accepting group should result in more back-transfer upon MMLL′CT excitation. Moreover, oscillator strength for Pt complexes is larger than for Pd ones, as our theoretical results have shown. This, combined with larger λ_{max} values for the former, leads to materials with higher hyperpolarizability. Eisenberg *et al.*[2g] showed this experimentally using EFISH (electric field induced second harmonic) experiments on the compounds M(dpphen)(tbcda) and M(dpphen)(mncda), with M = Pd, Pt. Pt, as we previously discussed, gave better overlap due to its radial extensive orbital nature.

2.3. Triplet States and Emission Spectra. Most of the assignments of excited states and electronic transitions in (diimine)Pt(dithiolate) complexes are based on emission studies[2f,g,i,k−o,q−s] since the collected data, such as emission lifetimes, quantum yields, etc., allow easy discrimination between intra ligand ($\pi \rightarrow \pi$*) and charge transfer excited states. According to them, the major band originates from the closely spaced spin−orbit components of a state of [Pt/dithiolate → diimine] character, but of triplet multiplicity. In other words, absorption and emission arise from states of common nature. This is pretty applicable for most Pt(diimine)(dithiolate) complexes, but the 1,2-dithiolates with good π*-accepting electrons substitute. Actually there are two references up to now, Pt(diimine)(mnt)[2n] and Pt(dmbpy)-

(30) (a) Moylan, C. R.; Twieq, R. J.; Lee, V. Y.; Swanson, S. A.; Betterton, K. M.; Miller, R. D. *J. Am. Chem. Soc.* **1993**, *115*, 12599−12600. (b) Lees, A. J. *Comments Inorg. Chem.* **1995**, *17*, 319−342.
(31) Oudar, J. L.; Chemla, D. S. *J. Chem. Phys.* **1977**, *66*, 2664−2668.

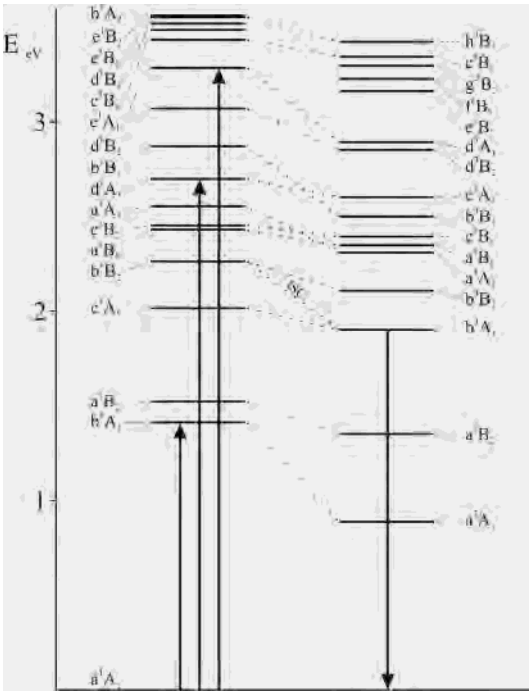

Figure 7. Singlet and triplet excited state diagrams of **3** as calculated by TDDFT. The correlation shown between singlet and triplet states is based on the principal contributing orbital excitation.

(met),[2r] which denote that the observed band originates from a state of [Pt/dithiolate → dithiolate] character. Herein we shall try to use both emission spectra in low-temperature solvent glasses and TDDFT calculations to probe for any difference in excited state properties between the two metals, namely, Pt and Pd, on one side and dithiolate derivatives on the other. To the best of our knowledge, only a few times before TDDFT triplet calculations have been employed in order to provide a reasonable interpretation of photophysical properties of metal complexes.[9]

Emission spectra were recorded for all complexes in a 1:1:1 DMSO:dichloromethane:methanol (DMM) glass at 77 K, under which conditions they are virtually photostable. Table 4 shows the maxima of the lowest-energy absorption and of the emission. None of the Pd complexes showed luminescence under these conditions in accordance with previous references.[22b] For reasons that are not fully understood, only some Pt(diimine)(dithiolate) complexes have been found to exhibit long-lived emission spectra. The latter one could be attributed to strong interactions with solvent in the case of Pd complexes which could play an important role in nonradiative decay. Alternatively, the less metal character in ligand−metal orbital mixing for Pd may facilitate a less partial delocalization across the metal center (compared to Pt), giving the complex some less extent of π-delocalization character. In this case, the lowest triplet component of this charge transfer is presumably buried in the broad absorption band, remains elusive, and has never been directly identified in absorption or excitation spectra.

In Figure 7 a singlet and triplet low energy excited state diagram of **3** is displayed, as representative of the other complexes. The correlation shown between singlet and triplet states is based on the principal contributing orbital excitation.

Proceeding to our analysis, two major points must be kept in mind. First as our experimental results pointed out, the main emission band of **4** arises on higher energy than the corresponding bands of **3** and **5**. Second, it has been verified that the emission band of **4** comes from a state of ^{3}[mnt/Pt → mnt] character (Table 9). More precisely, valence orbitals of **4** reveal that the first unoccupied orbital localized on the dithiolate is LUMO+4 ($9a_2$), whereas the LUMO+3 orbital ($33b_2$) is localized on both Pt and the dithiolate. As the next orbitals, localized on mnt, lie at quite high energy, they are not included in the following discussion. Based on the above clues, we may state that the most probable emitting triplet state of Pt(bpy)(mnt) is $c^1A_1 \rightarrow b^3B_2$ since the excitation occurs on the absorption band and satisfies the energy gap (2.22 eV). This value is justified as very satisfactory compared to the experimental one of 1.99 eV, considering the neglect of medium effects. On the other hand, the present employment of the TDDFT formalism does not include the treatment of spin−orbit coupling, which in the case of the third row transition metals would lower the predicted triplet states energy through interactions with higher singlet and triplet states by an amount of 0.2−0.3 eV.

The aforementioned pattern is slightly different for **3** and **5**. As we have already shown, a lower energy for the emission band exists (Table 4) as compared to **4**. So, the only possible transition for **5** is $c^1A_1 \rightarrow a^3B_2$, intersystem crossing, which is also energetically favored (Table 10). Moreover, a^3B_2 has ^{3}[edt/Pt → bpy] character in total consistency with the experimentally derived conclusions. For **3** the only permutable transition is the intersystem crossing $b^1B_2 \rightarrow b^3A_1$. Thus the emitting state is the triplet dithiolate/metal in character b^3A_1 state. The accuracy of our calculations is within the same magnitude as previously reported for **4**.

Conclusions

In this work we report the synthesis, characterization, and crystallographic data of Pd(phen)(bdt) (**1**) complex. Its properties are compared to those of other M(diimine)-(dithiolate) complexes. The ground-state structures of the complexes **1**, Pd(bpy)(bdt) (**2**), Pt(bpy)(bdt) (**3**), Pt(bpy)(mnt) (**4**), and Pt(bpy)(edt) (**5**) as calculated by B3LYP density functional calculations are in good agreement with available crystallographic studies. The highest occupied orbitals are dithiolate in character, but with almost equal admixture of diimine ligand and metal, consistent with π*-back-bonding theory. The nature of the lowest unoccupied orbital is mainly diimine, but there is also an admixture of metal and dithiolate, which is enlarged in the presence of Pt. Through DFT calculations, it has been demonstrated that the metal ion contributes to the Kohn−Sham HOMO through its *n*d atomic orbital ($n = 4, 5$ for Pd, Pt), which depends on *n*. Moreover since the only variable that distinguishes **2** and **3** is the identity of the metal atom, both theoretical and experimental results strongly support the idea that orbitals on the metal atom make a significant contribution to the HOMO of these systems. Considering the above-mentioned clues, the lowest-energy transition can be characterized as MMLL′CT.

The observed stabilization of the HOMO and LUMO of **4** is attributed to the π*-electron acceptor substituent of dithiolate ligand, namely, −CN.

Excited singlet and triplet states are examined using time dependent density functional theory (TDDFT). Optical spectra and solvatochromism of complexes **1**−**5** are attempted to be assigned using the aforementioned formalism. All the low lying transitions are categorized as "mixed-metal/ligand-to-ligand charge transfer" (MMLL′CT) in total accordance with the experimental work of Eisenberg and coworkers.[2] The emitting states of **3**, **4**, and **5** are attributed to b^3A_1 (2.02 eV), b^3B_2 (2.22 eV), and a^3B_2 (1.94 eV), respectively, consistent with symmetry and energy rules. The theoretical values are pretty well correlated to the experimental ones, assuming the lack of spin−orbit coupling in these TDDFT calculations and that the calculations are performed on gas-phase neglecting the solvents' effect.

Acknowledgment. We thank the Special Research Account of Athens University for partial support. Appreciation is expressed to Dr. D. Fox from Gaussian Inc., Prof. J. Fabian, Prof. C. Lauterbach, Prof A. Vlček, Jr., the researchers of the NRF, A. Avramopoulos, and D. Liakos for their precious help and to the reviewers for their valuable suggestions. C. Makedonas also thanks the Academy of Athens for support. The generous computing time offered by the National Center for Scientific Research, DEMOKRITOS, is greatly appreciated.

Supporting Information Available: Crystallographic data in CIF format. Tables of selected TDDFT calculated energies and compositions of the lowest lying singlet and triplet energy states of **1**−**4**. This material is available free of charge via the Internet at http://pubs.acs.org.

IC034978J